

# First search for $\alpha$ decays of naturally occurring Hf nuclides with emission of $\gamma$ quanta

F.A. Danevich<sup>a,1</sup>, M. Hult<sup>b</sup>, D.V. Kasperovych<sup>a</sup>, G.P. Kovtun<sup>c,d</sup>, K.V. Kovtun<sup>e</sup>,  
G. Lutter<sup>b</sup>, G. Marissens<sup>b</sup>, O.G. Polischuk<sup>a</sup>, S.P. Stetsenko<sup>c</sup>, V.I. Tretyak<sup>a</sup>

<sup>a</sup>*Institute for Nuclear Research, 03028 Kyiv, Ukraine*

<sup>b</sup>*European Commission, Joint Research Centre, Retieseweg 111, 2440 Geel, Belgium*

<sup>c</sup>*National Scientific Center Kharkiv Institute of Physics and Technology, 61108 Kharkiv, Ukraine*

<sup>d</sup>*Karazin Kharkiv National University, 61022 Kharkiv, Ukraine*

<sup>e</sup>*Public Enterprise "Scientific and Technological Center Beryllium", 61108 Kharkiv, Ukraine*

## Abstract

The first ever search for  $\alpha$  decays to the first excited state in Yb was performed for six isotopes of hafnium (174, 176, 177, 178, 179, 180) using a high purity Hf-sample of natural isotopic abundance with a mass of 179.8 g. For  $^{179}\text{Hf}$ , also  $\alpha$  decay to the ground state of  $^{175}\text{Yb}$  was searched for thanks to the  $\beta$ -instability of the daughter nuclide  $^{175}\text{Yb}$ . The measurements were conducted using an ultra low-background HPGe-detector system located 225 m underground. After 75 d of data taking no decays were detected but lower bounds for the half-lives of the decays were derived on the level of  $\lim T_{1/2} \sim 10^{15} - 10^{18}$  a. The decay with the shortest half-life based on theoretical calculation is the decay of  $^{174}\text{Hf}$  to the first  $2^+$  84.3 keV excited level of  $^{170}\text{Yb}$ . The experimental lower bound was found to be  $T_{1/2} \geq 3.3 \times 10^{15}$  a.

*Keywords:* Alpha decay;  $^{174}\text{Hf}$ ,  $^{176}\text{Hf}$ ,  $^{177}\text{Hf}$ ,  $^{178}\text{Hf}$ ,  $^{179}\text{Hf}$ ,  $^{180}\text{Hf}$ , Low-background HPGe  $\gamma$  spectrometry

## 1 INTRODUCTION

Alpha decay is one of the most important topics of nuclear physics both from the theoretical and experimental points of view. The process played a crucial role in the development of nuclear models, since it offers information about the nuclear structure, the nuclear levels and the properties of nuclei. In the last two decades many experimental and theoretical studies have been performed to investigate very rare  $\alpha$  decays with long half-lives ( $10^{15} - 10^{20}$  a) or/and low branching ratios ( $10^{-3} - 10^{-8}$ ) (see review [1] and references therein). The progress has been become possible thanks to the substantial improvements in the experimental low-background techniques and underground location of the experimental set-ups.

Natural hafnium consists of 6 isotopes, all of them are theoretically unstable in relation to  $\alpha$  decay; the energy releases ( $Q_\alpha$ ) are in the range of 1.3 – 2.5 MeV (see Table 1). The  $\alpha$

---

<sup>1</sup>Corresponding author. *E-mail address:* danevich@kinr.kiev.ua (F.A. Danevich).

decay to the ground state (g.s.) of the daughter nuclide was experimentally observed only for  $^{174}\text{Hf}$  which has the biggest value of  $Q_\alpha = 2494.5$  keV. Riezler and Kauw detected the decay in 1959 with the half-life  $T_{1/2} = 4.3 \times 10^{15}$  a by using nuclear emulsions [4]. Then Macfarlane and Kohman measured the half-life as  $T_{1/2} = 2.0(4) \times 10^{15}$  a with the help of an ionization chamber [5]. It should be noted that both the experiments utilized samples of enriched  $^{174}\text{Hf}$  (10.14% in both cases). The exposure in the experiments for the isotope  $^{174}\text{Hf}$  was  $0.0068$  g $\times$ d [4] and  $0.12$  g $\times$ d [5], respectively. The half-life value obtained in [5] is accepted currently as the recommended half-life of  $^{174}\text{Hf}$  [6].

Table 1: Characteristics of (potential)  $\alpha$  decays of hafnium isotopes.  $\delta$  is the isotopic abundance of the nuclide in the natural isotopic composition of elements.  $Q_\alpha$  value is given for the g.s. to g.s. transitions. Number of nuclei of the isotope of interest in the hafnium sample used in the present study is denoted as  $N$ .

Transition	$\delta$ [2]	$Q_\alpha$ (keV) [3]	$N$
$^{174}\text{Hf} \rightarrow ^{170}\text{Yb}$	0.0016(12)	2494.5(23)	$9.71 \times 10^{20}$
$^{176}\text{Hf} \rightarrow ^{172}\text{Yb}$	0.0526(70)	2254.2(15)	$3.19 \times 10^{22}$
$^{177}\text{Hf} \rightarrow ^{173}\text{Yb}$	0.1860(16)	2245.7(14)	$1.13 \times 10^{23}$
$^{178}\text{Hf} \rightarrow ^{174}\text{Yb}$	0.2728(28)	2084.4(14)	$1.65 \times 10^{23}$
$^{179}\text{Hf} \rightarrow ^{175}\text{Yb}$	0.1362(11)	1807.7(14)	$8.26 \times 10^{22}$
$^{180}\text{Hf} \rightarrow ^{176}\text{Yb}$	0.3508(33)	1287.1(14)	$2.13 \times 10^{23}$

In addition to  $\alpha$  decay to the ground state, all the isotopes can decay to excited levels of the daughter nuclei. In the latter processes the deexcitation  $\gamma$  quanta are emitted, which can be searched for by low-background  $\gamma$ -ray spectrometry. Because of the exponential dependence of the half-life on the decay energy [according to the Geiger-Nuttall law  $T_{1/2} \sim \exp(Q_\alpha^{-1/2})$ ] it is experimentally difficult to search for decay branches with low  $Q_\alpha$ -value. Therefore, in this work, we look for transitions only to the first excited levels of the daughter Yb nuclides. However, in case of the decay  $^{179}\text{Hf} \rightarrow ^{175}\text{Yb}$ , the  $^{175}\text{Yb}$  daughter is unstable. It beta decays to  $^{175}\text{Lu}$  ( $T_{1/2} \approx 4.2$  d and  $Q_\beta = 470$  keV) with the emission of gamma quanta, being the most intensive one with  $E_\gamma = 396.3$  keV [7]. Thus, also  $^{179}\text{Hf}$  decay to the ground state of  $^{175}\text{Yb}$  can be looked for in such an approach. The simplified decay schemes of Hf  $\alpha$  decays are shown in Fig. 1.

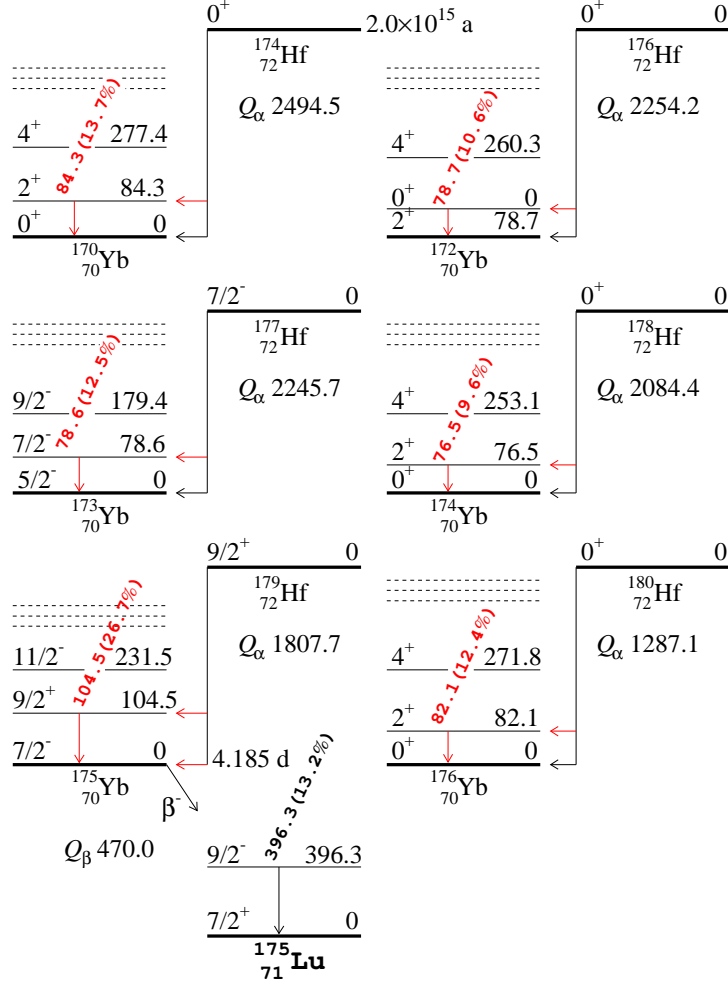


Figure 1: (Color online) Expected schemes of  $\alpha$  decay of the naturally occurring hafnium isotopes (levels above the second excited levels are omitted). The  $Q_\alpha$  values, energies of the levels and of the de-excitation  $\gamma$  quanta are given in keV, the probabilities of  $\gamma$  quanta emission are given in parentheses. Red arrows show transitions investigated in this work.

In this work, a search for  $\alpha$  decays accompanied by gamma-ray emission of six naturally occurring Hf isotopes was conducted. A specially purified hafnium sample (179.8 g) of natural isotopic abundance was measured in a HPGe-detector system located 225 m underground in the laboratory HADES (Belgium). The obtained  $T_{1/2}$  limits are compared with theoretical predictions based on a few theoretical models [8, 9, 10, 11].

## 2 EXPERIMENT

### 2.1 Sample of hafnium

A disc-shaped sample of metallic hafnium with diameter of 59.0 mm and 5.0 mm height, with the mass of 179.8 g, was used in the low-background experiment. The hafnium was obtained by reduction process from hafnium tetrafluoride with metallic calcium. Then the material was

additionally purified by double melting in vacuum by electron beam.

The purity of the obtained hafnium was measured by the Laser Ablation Mass Spectrometry as  $\simeq 99.8\%$ . It should be stressed that zirconium is typically the main contaminant of hafnium (in our case the mass concentration of Zr is  $0.4\%$ ). However, the purity level of Hf is usually given without taking into account the Zr contamination. The concentrations (limits) of other metal and gaseous impurities in the sample were on the level of  $0.005 - 0.05\%$  ( $\approx 0.2\%$  in total). The summary of the impurities detected (or their limits) in the Hf sample is presented in Table 2.

Table 2: Impurities detected (bounded) in the Hf sample by the Laser Ablation Mass Spectrometry.

Element	Mass concentration (%)
C	< 0.01
N	< 0.005
O	< 0.05
Mg	< 0.004
Al	< 0.005
Si	< 0.005
Ca	0.01
Ti	< 0.005
Cr	< 0.003
Mn	< 0.0005
Fe	0.04
Ni	0.02
Cu	< 0.005
Zr	0.4
Nb	0.01
Mo	0.01
W	0.01

## 2.2 Gamma-ray spectrometry set-ups

The experiment was realized with the help of two set-ups with three HPGe detectors (named Ge6, Ge7, and Ge10) at the HADES underground laboratory (Geel, Belgium) located at depth of 225 m below the ground. A schematic view of the set-ups is given in Fig. 2. The main characteristics of the detectors are presented in Table 3 (more details one can find in Refs. [12, 13]). First the Hf sample was stored 13 d underground to enable decay of short-lived cosmogenic radionuclides. The first measurement in which the sample was installed directly on the endcap of the detector Ge10 lasted 40.4 d (the set-up I, see Fig. 2). The Ge10 detector is perfect for looking for low-energy  $\gamma$ -rays (the effects searched for) taking into account its excellent energy resolution and high detection efficiency to low-energy  $\gamma$  quanta. Then the experiment was continued with the Ge6 detector instead of Ge10 for 34.8 d (set-up II). The Ge6 detector has a higher detection efficiency to middle-energy and high-energy  $\gamma$  quanta thanks

to a bigger volume and was used in the 2nd stage of the experiment to investigate in wider energy range radioactive contamination of the Hf sample thoroughly. The endcap height of the Ge10 detector is lower than that of Ge6. Therefore Ge7 was slightly (1.1 mm) further away from the sample in the set-up I compared to the set-up II. This consequently resulted in a higher detection efficiency of the detector Ge7 in the set-up II (see Table 5 in Section 3.2). The total exposure of the experiment is  $42 \text{ g} \times \text{d}$  for the isotope  $^{174}\text{Hf}$  (the exposure was calculated as a product of the  $^{174}\text{Hf}$  isotope mass in the sample and of the sum of the four measuring times of the detectors).

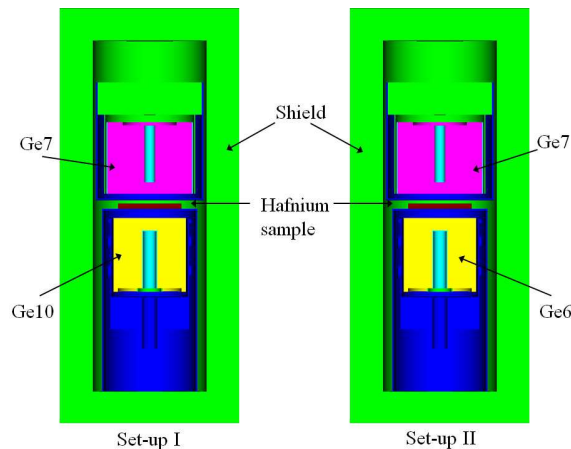


Figure 2: (Color online) Schematic view of the two low-background set-ups with HPGe detectors and hafnium sample.

Table 3: Properties of the HPGe detectors used in this study.

	Ge6	Ge7	Ge10
Energy resolution (FWHM) at 84 keV	1.4 keV	1.3 keV	0.9 keV
FWHM at 396 keV	1.8 keV	1.5 keV	1.2 keV
FWHM at 1332 keV	2.3 keV	2.2 keV	1.9 keV
Relative efficiency	80%	90%	62%
Crystal mass	2096 g	1778 g	1040 g
Window material and thickness	LB Cu 1.0 mm	HPAl 1.5 mm	HPAl 1.5 mm
Top dead layer thickness	0.9 mm	0.3 $\mu\text{m}$	0.3 $\mu\text{m}$

LB Cu = Low Background Copper

HPAl = High Purity Aluminum

## 3 RESULTS AND DISCUSSION

### 3.1 Radioactive impurities in the hafnium sample

Energy spectra recorded by the HPGe detectors with the hafnium sample and without sample (background) are presented in Fig. 3 (set-up I) and Fig. 4 (set-up II). The gamma peaks identified in the spectra belong mainly to the naturally occurring primordial radionuclides:  $^{40}\text{K}$ , and daughters of the  $^{232}\text{Th}$ ,  $^{235}\text{U}$ , and  $^{238}\text{U}$  families. There is statistically significant excess in the peaks of  $^{228}\text{Ac}$  (in equilibrium with  $^{228}\text{Ra}$  from the  $^{232}\text{Th}$  family),  $^{235}\text{U}$ ,  $^{231}\text{Pa}$ ,  $^{227}\text{Ac}$  (daughters of  $^{235}\text{U}$ ),  $^{234m}\text{Pa}$  and  $^{226}\text{Ra}$  ( $^{238}\text{U}$ ) in the data collected with the sample. In addition, we have observed in the hafnium sample two cosmogenic (neutron induced) radionuclides  $^{175}\text{Hf}$  [decays by electron capture with  $Q_{EC} = 683.9(20)$  keV and half-life  $T_{1/2} = 70(2)$  d] and  $^{181}\text{Hf}$  [beta active with  $Q_{\beta} = 1035.5(18)$  keV,  $T_{1/2} = 42.39(6)$  d]. It should be stressed that the counting rate in the  $\gamma$  peaks of  $^{175}\text{Hf}$  and  $^{181}\text{Hf}$  became substantially lower in the later measurements in the set-up II due to decay in the underground conditions.

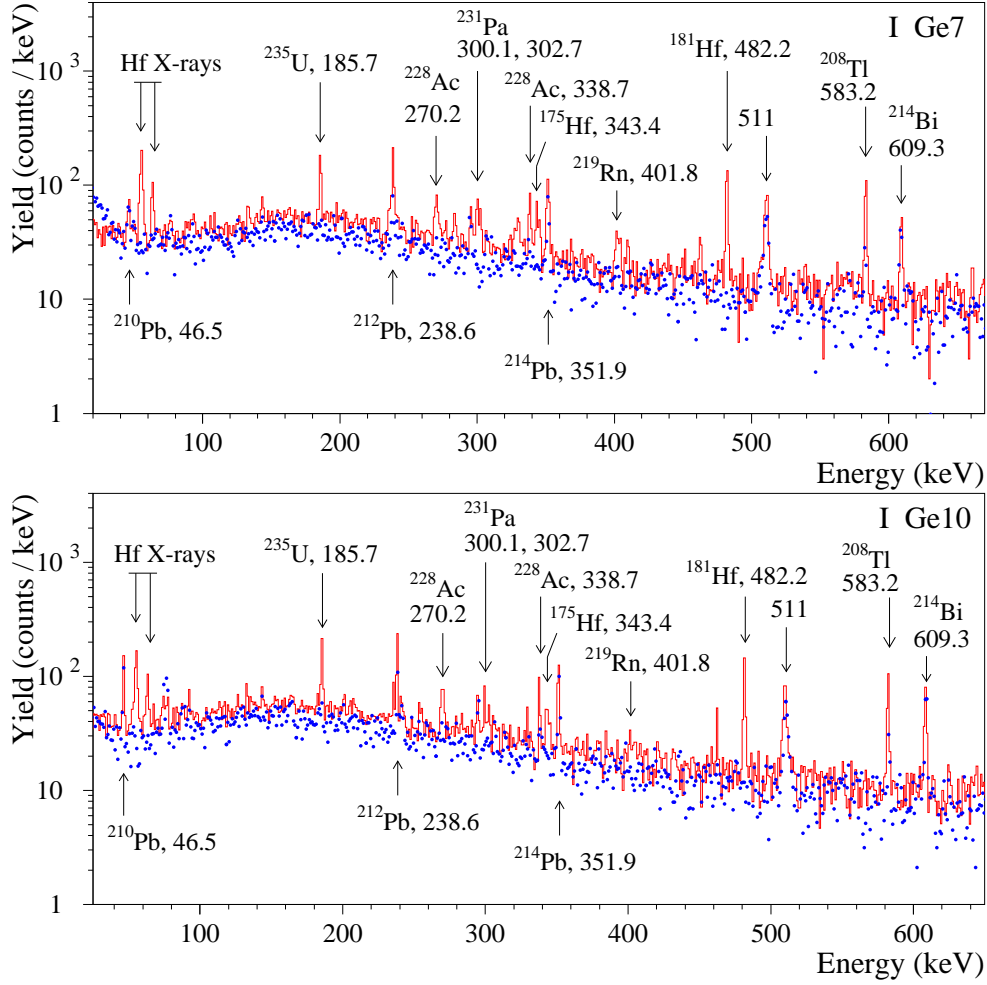


Figure 3: (Color online) Energy spectra accumulated with the hafnium sample (solid line) and without sample (dots) by ultra-low-background HPGGe  $\gamma$  detectors Ge7 (over 38.4 d with the hafnium sample and over 38.5 d without sample), and Ge10 (over 40.4 d with hafnium and 38.5 d background). The background energy spectra are normalized to the times of measurements with the Hf sample. Energy of  $\gamma$  lines are in keV.

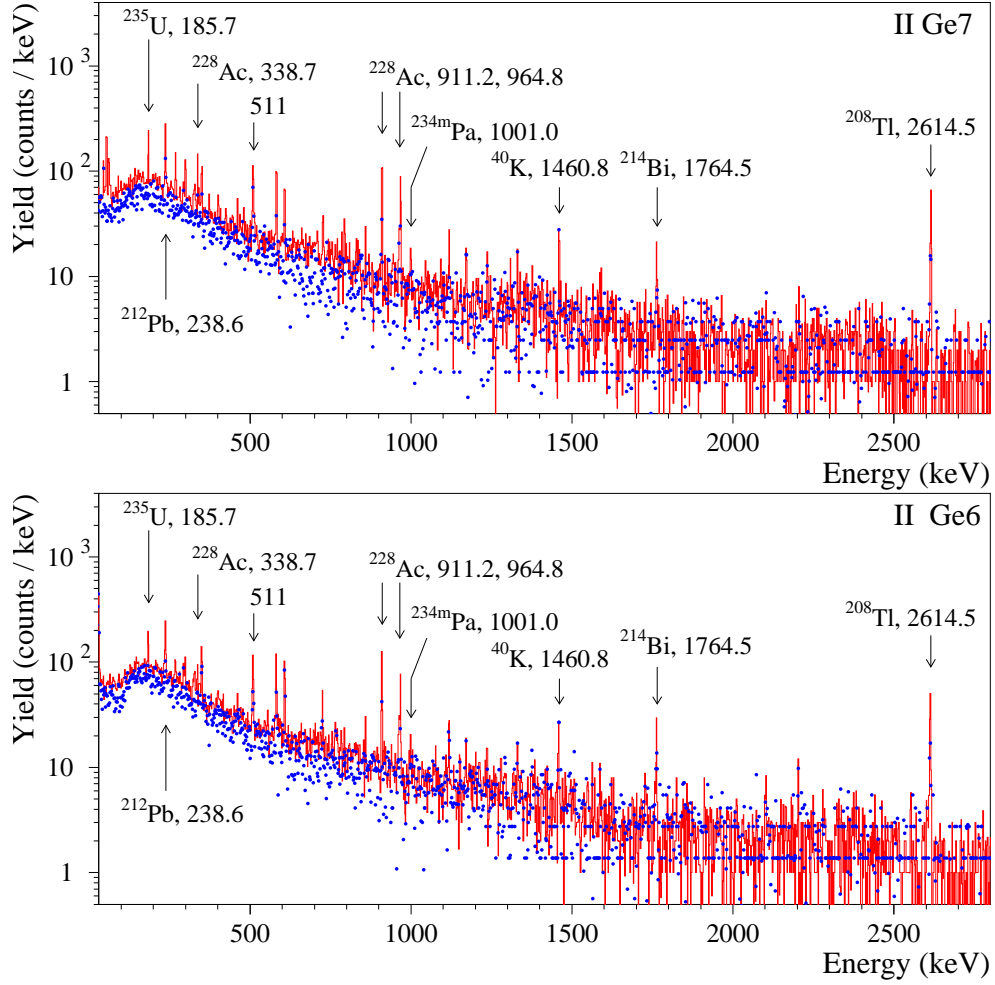


Figure 4: (Color online) Energy spectra accumulated with the hafnium sample (solid line) and without sample (dots) by ultra-low-background HPGGe  $\gamma$  detectors Ge7 (over 34.8 d with the hafnium sample and over 28.1 d without sample) and Ge6 (over 34.8 d with hafnium and 25.3 d background). The background energy spectra are normalized to the times of measurements with the Hf sample. Energy of  $\gamma$  lines are in keV.



Massic activities of the radionuclides in the hafnium sample were calculated with the formula:

$$A = (S_{sample}/t_{sample} - S_{bg}/t_{bg})/(\eta \cdot \varepsilon \cdot m) \quad (1)$$

where  $S_{sample}$  ( $S_{bg}$ ) is the area of a peak in the sample (background) spectrum;  $t_{sample}$  ( $t_{bg}$ ) is the time of the sample (background) measurement;  $\eta$  is the  $\gamma$ -ray emission intensity of the corresponding transition [14];  $\varepsilon$  is the full energy peak efficiency;  $m$  is the mass of the sample. The detection efficiencies were calculated with EGSnrc simulation package [15, 16], the events were generated homogeneously in the Hf sample. The calculations were validated in the measurements with  $^{109}\text{Cd}$  and  $^{133}\text{Ba}$   $\gamma$  sources (set-up I), and  $^{109}\text{Cd}$ ,  $^{133}\text{Ba}$ ,  $^{134}\text{Cs}$ ,  $^{152}\text{Eu}$ , and  $^{241}\text{Am}$  sources (set-up II). The standard deviation of the relative difference between the simulations and the experimental data is 5 – 7% for  $\gamma$  peaks in the energy interval 53.2 keV – 383.8 keV for the set-up I, and is 6% for  $\gamma$  peaks in the energy interval 59.5 keV – 1408.0 keV for the set-up II.

A clear excess of the count-rate in the energy spectra gathered with the Hf sample observed for  $\gamma$  peaks of  $^{228}\text{Ac}$  (in equilibrium with  $^{228}\text{Ra}$ ),  $^{212}\text{Pb}$ ,  $^{212}\text{Bi}$  and  $^{208}\text{Tl}$  ( $^{228}\text{Th}$ ) allows to estimate the massic activities in the sample of  $^{228}\text{Ra}$  ( $20 \pm 4$  mBq/kg) and  $^{228}\text{Th}$  ( $13.3 \pm 1.4$  mBq/kg). No wonder that the equilibrium of the  $^{232}\text{Th}$  chain is broken: the chemical properties of radium and thorium are rather different.

A massic activity of  $^{238}\text{U}$  was estimated on the basis of  $^{234m}\text{Pa}$   $\gamma$  peak with energy 1001.0 keV as  $59 \pm 28$  mBq/kg. Some excess of  $^{214}\text{Pb}$  and  $^{214}\text{Bi}$   $\gamma$ -peaks areas was observed in the energy spectra accumulated with the Hf sample. Assuming the  $^{226}\text{Ra}$  sub-chain in equilibrium,  $^{226}\text{Ra}$  massic activity can be calculated as  $1.6 \pm 1.3$  mBq/kg. It should be stressed, however, that the measurements were not carried out in a radon-tight container. Thus, we give conservatively a limit on the  $^{226}\text{Ra}$  massic activity in the sample:  $\leq 3.7$  mBq/kg. The substantially smaller activity of  $^{226}\text{Ra}$  in comparison to its mother  $^{238}\text{U}$  can be explained by a broken equilibrium of the  $^{238}\text{U}$  chain occurred in the hafnium sample production process, also a quite expectable case taking into account the rather different chemical properties of uranium and radium. We cannot conclude that the  $^{210}\text{Pb}$  sub-chain is out of equilibrium too. However, the sensitivity of the set-ups to  $^{210}\text{Pb}$  is rather limited due to the low detection efficiency and small  $\gamma$ -ray emission intensity of the 46.5 keV gamma quanta of  $^{210}\text{Pb}$  (4.25%).

A significant deviation of the  $^{235}\text{U}/^{238}\text{U}$  activities ratio [the ratio is 0.36(18)] from the expected one (0.046, assuming the natural isotopic abundance of the uranium isotopes) was observed in the Hf sample. An explanation for this could be that the production of the high pure hafnium tetrafluoride included centrifugation of gaseous Hf compound to reduce zirconium concentration. The contamination by  $^{235}\text{U}$  could occur due to proximity between the industrial sites of the centrifugation facilities to purify hafnium and to enrich uranium by the Soviet Union industry. The details of the Hf production process are unknown, however, this explanation of the  $^{235}\text{U}/^{238}\text{U}$  ratio deviation looks a most reasonable one.

If no statistically significant peak excess was detected (the cases of  $^{40}\text{K}$ ,  $^{60}\text{Co}$ ,  $^{137}\text{Cs}$ ,  $^{178m2}\text{Hf}$ ,  $^{182}\text{Hf}$ ), we set limits on massic activities of possible radioactive impurities in the sample. The calculated massic activities (limits) of radioactive impurities in the Hf sample are summarized in Table 4. Only one unidentified peak with energy 1310.6(4) keV and area 14(4) counts was observed in the energy spectrum of the Ge7 detector measured with the Hf sample in the set-up II.

Table 4: Radioactive contamination of the Hf sample measured in HADES by HPGe  $\gamma$ -ray spectrometry. The massic activities of  $^{175}\text{Hf}$  and  $^{181}\text{Hf}$  are given with reference date at the start of each measurement for the set-up I and the set-up II (within brackets) separately. The upper limits are given at 90% C.L., the reported uncertainties are the combined standard uncertainties.

Chain	Nuclide	Massic activity (mBq/kg)	Activity in the sample (mBq)
	$^{40}\text{K}$	$\leq 8$	$\leq 1.4$
	$^{60}\text{Co}$	$\leq 0.6$	$\leq 0.11$
	$^{137}\text{Cs}$	$\leq 1.1$	$\leq 0.20$
	$^{172}\text{Hf}$	$\leq 17$	$\leq 3$
	$^{175}\text{Hf}$	$2.5 \pm 0.3$ ( $1.0 \pm 0.2$ )	$0.44 \pm 0.05$ ( $0.18 \pm 0.04$ )
	$^{178m2}\text{Hf}$	$\leq 0.4$	$\leq 0.06$
	$^{181}\text{Hf}$	$8.1 \pm 0.4$ ( $0.6 \pm 0.2$ )	$1.45 \pm 0.07$ ( $0.12 \pm 0.04$ )
	$^{182}\text{Hf}$	$\leq 2.8$	$\leq 0.5$
$^{232}\text{Th}$	$^{228}\text{Ra}$	$20 \pm 4$	$3.6 \pm 0.7$
	$^{228}\text{Th}$	$13.3 \pm 1.4$	$2.38 \pm 0.25$
$^{235}\text{U}$	$^{235}\text{U}$	$21 \pm 3$	$3.8 \pm 0.5$
	$^{231}\text{Pa}$	$60 \pm 19$	$11 \pm 3$
	$^{227}\text{Ac}$	$11 \pm 3$	$2.0 \pm 0.5$
$^{238}\text{U}$	$^{234m}\text{Pa}$	$59 \pm 28$	$11 \pm 5$
	$^{226}\text{Ra}$	$\leq 3.7$	$\leq 0.7$
	$^{210}\text{Pb}$	$\leq 280$	$\leq 50$

### 3.2 Search for $\alpha$ decay of $^{174}\text{Hf}$ to the first excited level of $^{170}\text{Yb}$

The energy release for  $^{174}\text{Hf}$   $Q_\alpha = 2494.5$  keV is the highest among the naturally occurring Hf nuclides, and its  $\alpha$  decay to the g.s. of  $^{170}\text{Yb}$  was already observed [4, 5] ( $T_{1/2} = 2.0 \times 10^{15}$  a). The energy of the first excited level of  $^{170}\text{Yb}$  daughter is quite low (84.3 keV), and the corresponding value of  $Q_\alpha^* = 2410.2$  keV is not far from that for the g.s. transition that gives a hope to observe this decay too. We pay a special attention to search for this process here.

There is no peak in any energy spectra that can be interpreted as  $\alpha$  decay of  $^{174}\text{Hf}$  to the 84.3 keV excited level of  $^{170}\text{Yb}$ <sup>2</sup>. Therefore we can set a lower half-life limit on the decay with the following formula:

$$\lim T_{1/2} = \ln 2 \cdot N \cdot \varepsilon \cdot \eta \cdot t / \lim S, \quad (2)$$

where  $N$  is the number of potentially  $\alpha$  unstable nuclei,  $\varepsilon$  is the detection efficiency,  $\eta$  is the 84.3 keV gamma-ray emission intensity (equal to 13.7% [6]),  $t$  is the measurements time, and  $\lim S$  is the number of events of the effect searched for which can be excluded at a given confidence level (C.L.; in the present work all the half-life limits are given with 90% C.L.). The detection efficiencies for different detectors were simulated with the help of the EGSnrc package [15, 16].

<sup>2</sup>In the spectrum of the detector Ge10 there is a structure near the energy of interest with an area  $20.2 \pm 10.2$  counts, that is no evidence of the effect searched for (see text below and Fig. 5).

To estimate the  $\lim S$  value, the energy spectra accumulated with the hafnium sample were fitted by a model consisting from the effect searched for (a Gaussian peak centered at 84.3 keV with the width determined for the each detector individually) and a first order polynomial function to describe continuous background. To extend the energy interval of fit (with an aim to improve description of the background) we have added in the model X-ray peaks. The X-rays can be caused by decays of  $^{232}\text{Th}$ ,  $^{235}\text{U}$  and  $^{238}\text{U}$  daughters in the sample and/or details of the experimental set-ups. The experimental spectra were fitted in the energy intervals within 70 – 80 keV, for the starting point, and 86 – 94 keV, for the final point, with a step of 1 keV. The best fits of the data obtained with the four detectors are shown in Fig. 5. The fits are characterized by the  $\chi^2/\text{n.d.f.}$  values (where n.d.f. is the number of degrees of freedom) within 0.54 – 0.93. The obtained areas of the peak are given in Table 5 together with the values of  $\lim S$  (calculated by using recommendations [17]), and the detection efficiencies for the 84.3 keV gamma quanta in each detector.

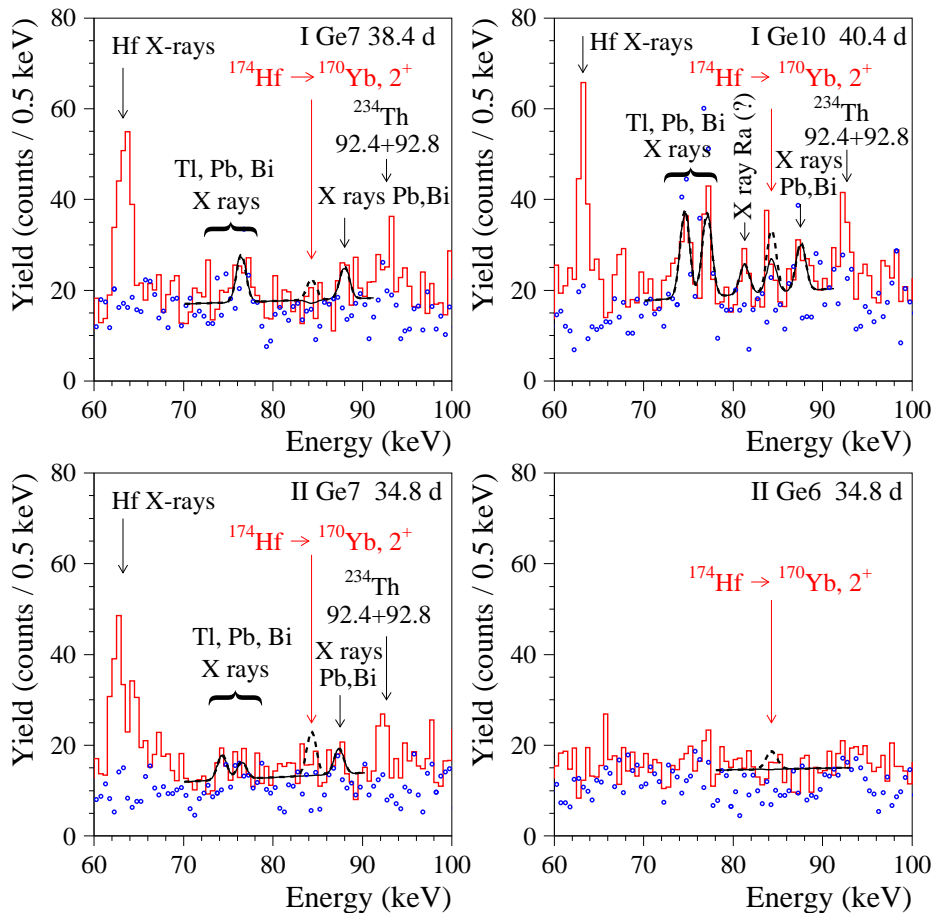


Figure 5: (Color online) Parts of the energy spectra accumulated with the hafnium sample in the set-ups I and II by the HPGe detectors (solid red histograms). The background energy spectra, normalized on the time of measurements with the sample, are depicted by blue dots. The models of the fits of the spectra with sample are shown by solid lines, while the peaks expected in  $\alpha$  decay of  $^{174}\text{Hf}$  to the  $2^+$  84.3 keV excited level of  $^{170}\text{Yb}$ , excluded with 90% C.L., are shown by dashed lines.

Table 5: Half-life lower limits on  $\alpha$  decay of  $^{174}\text{Hf}$  to the 84.3 keV excited level of  $^{170}\text{Yb}$  obtained from analysis of the data recorded with four HPGe detectors. The combined limit obtained by using Eq. (4) from the results of the individual spectra fits, and from the fit of the sum spectrum of the detector Ge7 in the set-ups I and II, and of the fit of sum spectrum of all four detectors are presented too (see text for details). All the limits are given at 90% C.L.

Set-up Detector	Time of measurements (d)	Number of counts in 84.3 keV peak	$\lim S$ (counts)	Detection efficiency	Half-life limit (a)
I Ge7	38.4	$-2.0 \pm 8.6$	12.2	0.005176	$4.1 \times 10^{15}$
I Ge10	40.4	$20.2 \pm 10.2$	36.9	0.004491	$1.2 \times 10^{15}$
II Ge7	34.8	$12.1 \pm 8.5$	26.0	0.005310	$1.8 \times 10^{15}$
II Ge6	34.8	$-0.3 \pm 7.5$	12.0	0.001251	$9.1 \times 10^{14}$
Combined all four detectors	148.4	$30.0 \pm 17.5$	58.7		$2.6 \times 10^{15}$
Combined I Ge7 + II Ge7	73.2	$10.1 \pm 12.1$	29.9		$3.2 \times 10^{15}$
Fit of sum spectrum of all four detectors	148.4	$29.8 \pm 17.4$	58.3		$2.6 \times 10^{15}$
Fit of sum spectrum I Ge7 + II Ge7	73.2	$9.8 \pm 11.5$	28.7		$3.3 \times 10^{15}$

As a next step, we tried to improve the experimental sensitivity by combining the data obtained with the different detectors. One can join results of several measurements by using the following formula:

$$T_{1/2} = \ln 2 \cdot N \cdot \eta \cdot \Sigma(\varepsilon_i \cdot t_i) / \Sigma S_i, \quad (3)$$

where  $\varepsilon_i$  are the detection efficiencies,  $t_i$  are the times of measurements for each detector,  $\Sigma S_i$  is the sum of events in the peak searched for in the data accumulated with the detectors. Since the effect is not observed, the formula is transformed to equation for a half-life limit and a limit on number of events as following:

$$\lim T_{1/2} = \ln 2 \cdot N \cdot \eta \cdot \Sigma(\varepsilon_i \cdot t_i) / \lim S, \quad (4)$$

where  $\lim S$  can be estimated by two approaches. First, one can calculate an arithmetic sum of the numbers of counts in the peak searched for, obtained from the fits of the individual spectra. One could expect that a highest sensitivity should be achieved by analysis of all the data of the detectors Ge6, Ge7 and Ge10 in the both set-ups. However, the analysis does not provide a highest sensitivity (see Table 5). It can be explained by the larger background in the sum spectrum and in average a lower detection efficiency (mainly of the detector Ge6 that has rather thick dead layer and thick copper endcap). The highest sensitivity was achieved by combining the peak areas obtained with the detector Ge7 in the set-ups I and II,  $S = 10.1 \pm 12.1$  counts, that results in the number of excluded events  $\lim S = 29.9$  counts (according to the recommendations [17]) and the half-life limit  $T_{1/2}({}^{174}\text{Hf}) \geq 3.2 \times 10^{15}$  a (at 90% C.L.).

Another way to estimate the value of  $\lim S$  is a fit of a sum spectrum of several detectors, taking into account a rather similar energy resolutions and the background conditions of the detectors. Again, the highest sensitivity was obtained not by the fit of all the sum spectra, but by the fit of the sum spectrum of the detector Ge7 in the set-ups I and II (see Table 5). The best fit was achieved in the energy interval 73 – 90 keV (with  $\chi^2/\text{n.d.f.} = 16.9/28 = 0.604$ ), providing the peak area  $S = 9.8 \pm 11.5$  counts that corresponds to the  $\lim S = 28.7$  counts. The fit and the excluded effect are shown in Fig. 6. Finally, we accept the result of the fit to derive the following limit on  $\alpha$  decay of  ${}^{174}\text{Hf}$  to the first excited level of  ${}^{170}\text{Yb}$  (at 90% C.L.):

$$T_{1/2}({}^{174}\text{Hf}) \geq 3.3 \times 10^{15} \text{ a}^3.$$

The obtained limit is still about two-three orders of magnitude lower than the theoretical estimations calculated by using the methods proposed in [8, 9, 10, 11] (see Section 3.4).

---

<sup>3</sup>One can see in Table 5 that the strongest half-life limit was obtained with the detector Ge7 in the set-up I. However, the large  $\lim T_{1/2}$  appears due to the negative peak area that results in a small  $\lim S$  value. We prefer to use the estimation obtained from the higher statistics acquired with the detector Ge7 in the set-ups I and II.

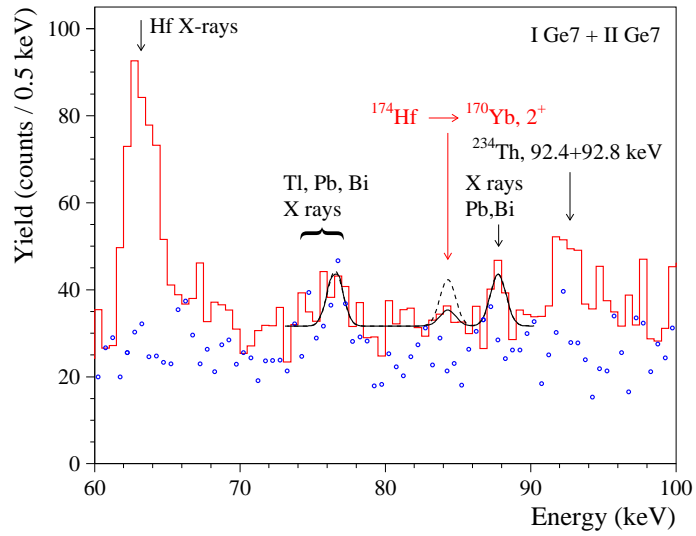


Figure 6: (Color online) Part of the sum energy spectrum accumulated with the hafnium sample in the set-ups I and II by the detector Ge7 over 73.2 d (solid red histogram), and the background spectrum of the detector for 66.6 d (normalized on the time of measurements with the sample, blue dots). Fit of the data with the sample is shown by solid line, while the excluded with 90% C.L. peak expected in the  $\alpha$  decay of  $^{174}\text{Hf}$  to the  $2^+$  84.3 keV excited level of  $^{170}\text{Yb}$  with an area of 28.7 counts is shown by dashed line.

### 3.3 Search for $\alpha$ decay of other hafnium isotopes

To estimate half-life limits for other naturally occurring hafnium nuclides relative to  $\alpha$  decay to the first excited levels of daughter nuclei, we have analyzed the individual spectra and different combinations of the energy spectra in the energy intervals where  $\gamma$  peaks after the  $\alpha$  decays are expected. The data on the parameters of the fits, excluded peaks areas and calculated half-life limits for  $^{176}\text{Hf}$ ,  $^{177}\text{Hf}$ ,  $^{178}\text{Hf}$ ,  $^{179}\text{Hf}$  and  $^{180}\text{Hf}$  are given in Table 6. Examples of the sum energy spectra fits for  $^{176}\text{Hf}$ ,  $^{179}\text{Hf}$  and  $^{180}\text{Hf}$  are presented in Fig. 7. As previously, the detection efficiencies were calculated with the EGSnrC simulation package. Gamma-ray emission intensities of  $\gamma$ 's expected in deexcitation processes, are taken as:  $^{176}\text{Hf} - \eta(\gamma \text{ 78.7 keV}) = 10.6\%$  [18];  $^{177}\text{Hf} - \eta(\gamma \text{ 78.6 keV}) = 12.5\%$  [19];  $^{178}\text{Hf} - \eta(\gamma \text{ 76.5 keV}) = 9.6\%$  [20];  $^{180}\text{Hf} - \eta(\gamma \text{ 82.1 keV}) = 12.4\%$  [21].

In possible  $\alpha$  decay of  $^{179}\text{Hf}$ , the  $^{175}\text{Yb}$  daughter nucleus is unstable. It decays through  $\beta^-$  decay to  $^{175}\text{Lu}$  with  $T_{1/2} = 4.2$  d and  $Q_\beta = 470.0$  keV emitting the most intensive  $\gamma$  quantum with  $E_\gamma = 396.3$  keV with yield of 13.2% [7]. Since the peak at 396.3 keV is not detected in the measured energy spectra, we set the following limit on  $^{179}\text{Hf}$   $\alpha$  decay half-life:  $T_{1/2} \geq 2.2 \times 10^{18}$  a. It should be stressed that the limit is valid also for  $\alpha$  decay of  $^{179}\text{Hf}$  to the ground state and for all the energetically allowed  $\alpha$  transitions to excited levels of  $^{175}\text{Yb}$ .

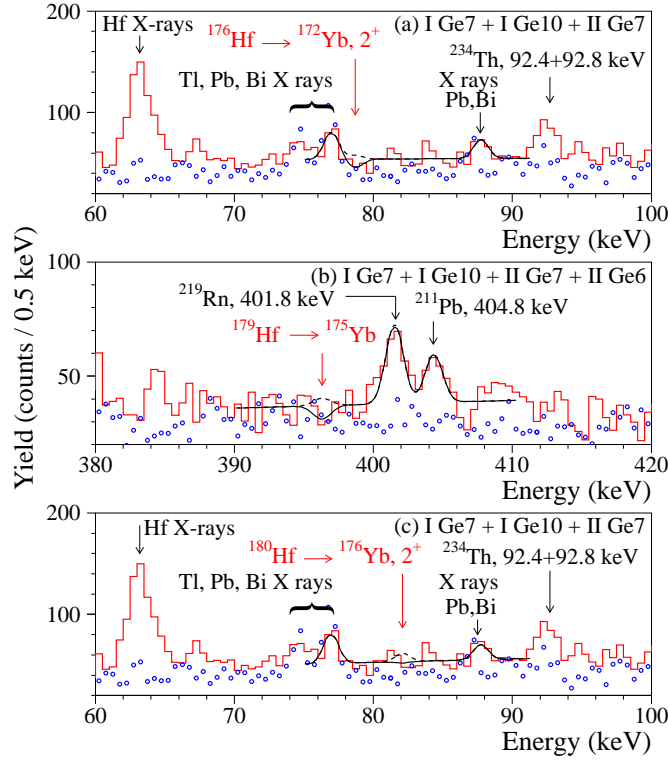


Figure 7: (Color online) Parts of the sum energy spectra accumulated with the hafnium sample by the detectors Ge7 (the set-ups I and II) and Ge10 (the set-up I) with the total measurement time 113.6 d (a and c), and of all four detectors over 148.4 d (b). The corresponding background spectra, normalized on the time of measurements with the Hf sample, are shown by blue dots. Fits of the data are shown by solid lines, while the excluded with 90% C.L. peaks expected in the  $\alpha$  decays of  $^{176}\text{Hf}$  (a),  $^{179}\text{Hf}$  (b) and  $^{180}\text{Hf}$  (c) are drawn by dashed lines.

Table 6: Half-life lower limits on  $\alpha$  decay of  $^{176}\text{Hf}$ ,  $^{177}\text{Hf}$ ,  $^{178}\text{Hf}$  and  $^{180}\text{Hf}$  to the first excited levels of the daughter Yb nuclei. Limit for  $^{179}\text{Hf}$  is valid for  $\alpha$  transitions to any of  $^{175}\text{Yb}$  levels, including the ground state. The limits are given at 90% C.L.

Transition	Method and data	Number of counts in the expected $\gamma$ peak (the $\gamma$ peak energy is given in parenthesis)	lim $S$ (counts)	Half-life limit (a)
$^{176}\text{Hf} \rightarrow ^{172}\text{Yb}$ 2 <sup>+</sup> 78.7 keV	Fit of sum spectra I Ge7, I Ge10, II Ge7	$-22.6 \pm 16.4$ (78.7 keV)	10.0	$3.0 \times 10^{17}$
$^{177}\text{Hf} \rightarrow ^{173}\text{Yb}$ 7/2 <sup>-</sup> 78.6 keV	Fit of sum spectra I Ge7, I Ge10, II Ge7	$-22.6 \pm 16.4$ (78.6 keV)	10.0	$1.3 \times 10^{18}$
$^{178}\text{Hf} \rightarrow ^{174}\text{Yb}$ 2 <sup>+</sup> 76.5 keV	Fit of sum of all four spectra	$-45.1 \pm 68.3$ (76.5 keV)	71.8	$2.0 \times 10^{17}$
$^{179}\text{Hf} \rightarrow ^{175}\text{Yb}$ all levels	Fit of sum of all four spectra	$-19.0 \pm 15.3$ (396.3 keV)	10.3	$2.2 \times 10^{18}$
$^{180}\text{Hf} \rightarrow ^{176}\text{Yb}$ 2 <sup>+</sup> 82.1 keV	Fit of sum spectra I Ge7, I Ge10, II Ge7	$-2.5 \pm 15.2$ (82.1 keV)	22.6	$1.0 \times 10^{18}$

### 3.4 Theoretical $T_{1/2}$ estimations

We calculated theoretical half-life values using 3 different approaches: (1) semiempirical formulae [8] based on the liquid drop model and the description of the  $\alpha$  decay as a very asymmetric fission process; (2) cluster model of [9, 10]; (3) semiempirical formulae [11]. These approaches were tested with known experimental half-lives of near four hundred  $\alpha$  emitters and demonstrated good agreement between calculated and experimental  $T_{1/2}$  values, mainly inside a factor of 2 – 3. No change in spin and parity in parent-to-daughter transition is supposed in calculations with [8, 9, 10]. So, in the cases, when such a difference existed and the emitted  $\alpha$  particle has non-zero angular momentum  $L$ , we took into account the additional hindrance factor, calculated in accordance with [22] (for the lowest possible  $L$  value). Denisov et al. [11] took non-zero  $L$  into account explicitly.

Table 7 summarizes the experimental half-life limits (lower bounds) obtained in this work as well as the half-life values obtained from the theoretical calculations.

## 4 CONCLUSIONS

A 179.8 g hafnium sample of natural isotopic abundance was measured using ultra low-background  $\gamma$ -ray spectrometry with the aim to search for  $\alpha$  decays of the naturally occurring hafnium isotopes to the first excited state of the daughter nuclei. For  $^{179}\text{Hf}$  also  $\alpha$  decay to the ground state of  $^{175}\text{Yb}$  was searched for thanks to the  $\beta$ -instability of the daughter nuclide  $^{175}\text{Yb}$ . None of the decays were detected but for the first time lower bounds were derived for these decays as reported in Table 7. One can note that among the different decays, it is the decay of  $^{174}\text{Hf}$  that has the experimental limit ( $3.3 \times 10^{15}$  a) which is closest to the lowest theoretical estimation



Table 7: Half-life limits on the  $\alpha$  decay of Hf isotopes in comparison with the theoretical predictions calculated here with approaches [8, 9, 10, 11]. The limits are given at 90% C.L.

Transition	Level of the daughter nucleus (keV)	Experimental $T_{1/2}$ (a)	Theoretical $T_{1/2}$ (a)		
			[8]	[9, 10]	[11]
$^{174}\text{Hf} \rightarrow ^{170}\text{Yb}$	$0^+$ , g.s.	$= 2.0(4) \times 10^{15}$ [5]	$7.4 \times 10^{16}$	$3.5 \times 10^{16}$	$3.5 \times 10^{16}$
	$2^+$ , 84.3	$\geq 3.3 \times 10^{15}$	$3.0 \times 10^{18}$	$1.3 \times 10^{18}$	$6.6 \times 10^{17}$
$^{176}\text{Hf} \rightarrow ^{172}\text{Yb}$	$2^+$ , 78.7	$\geq 3.0 \times 10^{17}$	$3.5 \times 10^{22}$	$1.3 \times 10^{22}$	$4.9 \times 10^{21}$
$^{177}\text{Hf} \rightarrow ^{173}\text{Yb}$	$7/2^-$ , 78.6	$\geq 1.3 \times 10^{18}$	$1.2 \times 10^{24}$	$9.1 \times 10^{21}$	$3.6 \times 10^{23}$
$^{178}\text{Hf} \rightarrow ^{174}\text{Yb}$	$2^+$ , 76.5	$\geq 2.0 \times 10^{17}$	$8.1 \times 10^{25}$	$2.4 \times 10^{25}$	$7.1 \times 10^{24}$
$^{179}\text{Hf} \rightarrow ^{175}\text{Yb}$	$(7/2^-)$ , g.s.	$\geq 2.2 \times 10^{18}$	$4.0 \times 10^{32}$	$4.4 \times 10^{29}$	$4.7 \times 10^{31}$
	$(9/2^+)$ , 104.5	$\geq 2.2 \times 10^{18}$	$2.5 \times 10^{35}$	$2.0 \times 10^{32}$	$2.2 \times 10^{34}$
$^{180}\text{Hf} \rightarrow ^{176}\text{Yb}$	$2^+$ , 82.1	$\geq 1.0 \times 10^{18}$	$4.1 \times 10^{50}$	$4.0 \times 10^{49}$	$2.1 \times 10^{48}$

( $6.6 \times 10^{17}$  a). There is a factor 200 between these two values. One cannot exclude that it is possible to conceive an experiment that succeeds in improving sensitivity by two orders of magnitude compared to these measurements. Solely by using a sample of the same mass but enriched to 10% (very expensive of course) one obtains a factor 60. By using HPGe detectors optimized for high resolution and low background in the 84 keV region (e.g. so-called BEGe-detectors) one possibly obtains another factor 2. Finally by increasing the measurement time from 2 months to one year one obtains another factor of 2.5 and in total one reaches a factor 300.

To go further one can go for a “source = detector” approach where the sample and detector are the same. As possible candidates, two new crystal scintillators can be named:  $\text{Cs}_2\text{HfCl}_6$  [23] and  $\text{Tl}_2\text{HfCl}_6$  [24]. The scintillating bolometer technique with simultaneous measurement of the heat and light signals seems to be the best choice ensuring high efficiency ( $\simeq 100\%$ ), good energy resolution (on the level of few keV), and possibility to distinguish between signals induced by  $\alpha$  and  $\beta(\gamma)$  particles. It would be also interesting to remeasure  $^{174}\text{Hf}$   $\alpha$  decay to the g.s. of  $^{170}\text{Yb}$  because  $\simeq 20 - 35$  factor difference between the experimental  $T_{1/2} = 2.0(4) \times 10^{15}$  a [5] and calculated  $T_{1/2} = (3.5 - 7.4) \times 10^{16}$  a [8, 9, 10, 11] is not usual for even-even nuclei (usually this difference is within a factor 2 - 3).

The limits obtained for other hafnium isotopes  $\lim T_{1/2} \sim 10^{17-18}$  a are very far from the theoretical predictions.

We have found the hafnium sample contaminated on the level of tens mBq/kg by  $^{232}\text{Th}$ ,  $^{235}\text{U}$  and  $^{238}\text{U}$  daughters. Deep purification of hafnium looks a rather complicated task, taking into account typically high contamination of hafnium by Th and U, and very high melting and boiling points of Hf (2227 °C and 4602 °C, respectively). The last circumstance provides certain difficulties to apply the efficient purification methods, like distillation, crystallization or zone melting. The observed in the sample cosmogenic  $^{175}\text{Hf}$  and  $^{181}\text{Hf}$  on the mBq/kg level are rather short-living (the half-lives are  $\simeq 70$  d and  $\simeq 42$  d, respectively). Therefore the contamination should not provide a substantial background after long enough (order of year) Hf cooling deep underground. It should be stressed, however, that the internal radioactive contamination of the Hf sample utilized in the present experiment does not restrict the present experiment sensitivity.

The main background was due to the naturally occurring trace radioactive contamination of the experimental set-ups. Nevertheless, advanced purification methods and enabling production of pure isotopically enriched  $^{174}\text{Hf}$ , without contamination by enriched  $^{235}\text{U}$ , would improve the background situation further.

## 5 ACKNOWLEDGMENTS

This project received support from the EC-JRC open access project EUFRAT under Horizon2020. The group from the Institute for Nuclear Research (Kyiv, Ukraine) was supported in part by the program of the National Academy of Sciences of Ukraine “Fundamental research on high-energy physics and nuclear physics (international cooperation)”. D.V.K. and O.G.P. were supported in part by the project “Investigations of rare nuclear processes” of the program of the National Academy of Sciences of Ukraine “Laboratory of young scientists” (Grant No. 0118U002328).

## References

- [1] P. Belli et al., Experimental searches for rare alpha and beta decays, *Eur. Phys. J. A* 55 (2019) 140.
- [2] J. Meija et al., Isotopic compositions of the elements 2013 (IUPAC Technical Report), *Pure Appl. Chem.* 88 (2016) 293.
- [3] M. Wang et al., The AME2016 atomic mass evaluation, *Chin. Phys. C* 41 (2017) 030003.
- [4] W. Riezler, G. Kauw, Natürliche Radioaktivität von Gadolinium 152 und Hafnium 174, *Z. Naturforsch.* 14a (1959) 196.
- [5] R.D. Macfarlane, T.P. Kohman, Natural alpha radioactivity in medium-heavy elements, *Phys. Rev.* 121 (1961) 1758.
- [6] C.M. Baglin et al., Nuclear Data Sheets for  $A = 170$ , *Nucl. Data Sheets* 153 (2018) 1.
- [7] M.S. Basunia, Nuclear Data Sheets for  $A = 175$ , *Nucl. Data Sheets* 102 (2004) 719.
- [8] D.N. Poenaru, M. Ivascu, Estimation of the alpha decay half-lives, *J. Physique* 44 (1983) 791.
- [9] B. Buck, A.C. Merchant, S.M. Perez, Ground state to ground state alpha decays of heavy even-even nuclei, *J. Phys. G* 17 (1991) 1223.
- [10] B. Buck, A.C. Merchant, S.M. Perez, Favoured alpha decays of odd-mass nuclei, *J. Phys. G* 18 (1992) 143.
- [11] V.Yu. Denisov, O.I. Davidovskaya, I.Yu. Sedykh, Improved parametrization of the unified model for  $\alpha$  decay and  $\alpha$  capture, *Phys. Rev. C* 92 (2015) 014602.
- [12] J.S.E. Wieslander et al., The Sandwich spectrometer for ultra low-level  $\gamma$ -ray spectrometry, *Appl. Rad. Isot.* 67 (2009) 731.

- [13] M. Hult et al., Comparison of background in underground HPGe-detectors in different lead shield configurations, *Appl. Radiat. Isot.* 81 (2013) 103.
- [14] R.B. Firestone et al., *Table of Isotopes*, 8th ed. (John Wiley, N.Y., 1996) and CD update (1998).
- [15] I. Kawrakow et al., The EGSnrc Code System: Monte Carlo simulation of electron and photon transport. Technical Report PIRS-701, National Research Council Canada (2017).
- [16] G. Lutter, M. Hult, G. Marissens, H. Stroh, F. Tzika, A gamma-ray spectrometry analysis software environment, *Appl. Rad. Isot.* 134 (2018) 200.
- [17] G.J. Feldman, R.D. Cousins, Unified approach to the classical statistical analysis of small signals, *Phys. Rev. D* 57 (1998) 3873.
- [18] B. Singh, Nuclear Data Sheets for  $A = 172$ , *Nucl. Data Sheets* 75 (1995) 199.
- [19] V.S. Shirley, Nuclear Data Sheets for  $A = 173$ , *Nucl. Data Sheets* 75 (1995) 377.
- [20] E. Browne, H. Junde, Nuclear Data Sheets for  $A = 174$ , *Nucl. Data Sheets* 87 (1999) 15.
- [21] M.S. Basunia, Nuclear Data Sheets for  $A = 176$ , *Nucl. Data Sheets* 107 (2006) 791.
- [22] K. Heyde, *Basic Ideas and Concepts in Nuclear Physics*, 2nd ed. (IoP Bristol, 1999).
- [23] A. Burger et al., Cesium hafnium chloride: A high light yield, non-hygroscopic cubic crystal scintillator for gamma spectroscopy, *Appl. Phys. Lett.* 107 (2015) 143505.
- [24] Y. Fujimoto et al., New intrinsic scintillator with large effective atomic number:  $Tl_2HfCl_6$  and  $Tl_2ZrCl_6$  crystals for X-ray and gamma-ray detections, *Sensors and Materials* 30(7) (2018) 1577.